Applied Physics Letters

Donor-doping and reduced leakage current in Nb-doped $Na_{0.5}Bi_{0.5}TiO_3$

Cite as: Appl. Phys. Lett. **106**, 102904 (2015); https://doi.org/10.1063/1.4914509
Submitted: 15 December 2014 • Accepted: 28 February 2015 • Published Online: 12 March 2015

Ming Li, Linhao Li, Jiadong Zang, et al.

Donor-doping and reduced leakage current in Nb-doped $Na_{0.5}Bi_{0.5}TiO_3$

Ming Li,[1] Linhao Li,[1] Jiadong Zang,[2] and Derek C. Sinclair[1,a)]
[1]*Department of Materials Science and Engineering, University of Sheffield, Sir Robert Hadfield Building, Mappin Street, Sheffield S1 3JD, United Kingdom*
[2]*Institute of Materials Science, Technische Universität Darmstadt, Alarich-Weiss-Str. 2, 64287 Darmstadt, Germany*

(Received 15 December 2014; accepted 28 February 2015; published online 12 March 2015)

Low levels of so-called "donor-doping" in titanate-based perovskite oxides such as La for Ba, Sr, and Nb for Ti in (Ba, Sr)TiO_3 can significantly reduce the resistivity of these typical (d^0) dielectric materials and expand application areas to positive temperature coefficient resistors, thermoelectrics, conductive wafers as thin film substrates, and solid oxide fuel cell anode materials. Here, we show low levels of Nb-doping ($\leq$1 at. %) on the Ti-site in the well-known lead-free piezoelectric perovskite oxide $Na_{0.5}Bi_{0.5}TiO_3$ (NBT) produces completely different behaviours whereby much higher resistivity is obtained, therefore indicating a different donor-doping (substitution) mechanism. There is a switch in conduction mechanism from oxygen-ions in undoped NBT with an activation energy (E_a) of <0.9 eV to electronic (band gap) conduction in 0.5–1 at. % Nb-doped NBT with $E_a \sim 1.5$–1.8 eV. This demonstrates the necessity of further systematic doping studies to elucidate the defect chemistry of NBT which is clearly different to that of (Ba,Sr)TiO_3. This defect chemistry needs to be understood if NBT-based materials are going to be manufactured on a large scale for commercial applications. This study also illustrates different donor-doping mechanisms to exist within the family of d^0 titanate-based perovskites. [http://dx.doi.org/10.1063/1.4914509]

Titanate-based (d^0) perovskite oxides (Ba,Sr)TiO_3 are an important family of ferroelectric materials that have been widely used as ceramic capacitor materials for over 50 years.[1] Their technical importance has led to extensive studies on the effect of so-called "donor" and "acceptor" doping on the electrical properties and the associated defect chemistry in these titanates.[2] This has resulted in improved dielectric performance via optimised manufacturing processes with lower cost as well as discovery of new electrical phenomena and new application areas. For example, acceptor doping (replacing a host ion with a dopant of lower valence) in $BaTiO_3$ can improve the resistance to reduction when fired at low oxygen partial pressure (pO_2),[3,4] thus making it possible to use base-metal electrodes (such as Ni and Cu) as compared to noble metals (such as Pt and Pd). This led to a revolution in the manufacturing of multilayer ceramic capacitor (MLCC) in the 1980s and 1990s.[5] On the other hand, low levels (typically <1 at. %) of donor-doping (replacing a host ion with a dopant of higher valence) such as La at the Ba-site or Nb at the Ti-site in $BaTiO_3$ can dramatically transform this dielectric material into a n-type semiconductor with room temperature (RT) resistivity <100 Ωcm.[6–8] This phenomenon has been explored to develop positive temperature coefficient resistors (PTCR).[8] For $SrTiO_3$, much lower resistivity (<0.01 Ωcm at RT) can be achieved by donor-doping.[9] Nowadays, highly conductive Nb-doped $SrTiO_3$ wafers are widely used as thin film substrates. The extremely high conductivity also makes donor-doped $SrTiO_3$ a promising candidate as an oxide-based thermoelectric material.[10] More recently, A-site deficient La-doped $SrTiO_3$ has been developed as a solid oxide fuel cell anode material.[11] Although debates on the origin(s) of the high conductivity remain,[12–14] it is clear that electrons are the dominating charge carrier.

We recently reported the d^0 perovskite titanate $Na_{0.5}Bi_{0.5}TiO_3$ (NBT) to behave very differently from (Ba,Sr)TiO_3.[15,16] Two types of electrically distinctive NBT compositions exist. One is close to stoichiometric NBT that exhibits near intrinsic (band gap) electronic conduction with an activation energy for conduction (E_a) $\sim$ 1.7 eV and is an excellent dielectric. The other type is Bi-deficient NBT compositions that exhibit high oxide-ion conductivity accompanied with a decrease of E_a to <0.9 eV and with a significant increase in conductivity by more than three orders of magnitude below 600 °C. The switch between electronic and ionic conduction in NBT is induced by low levels ($\leq$2 at. %) of A-site cation (Na and/or Bi) nonstoichiometry, which is dramatic and has not been observed in (Ba,Sr)TiO_3.

The influence of Na/Bi nonstoichiometry on the electrical and piezoelectric properties of NBT has been reported previously, but the defect chemistry has remained unclear.[17–24] We clarified the mechanisms behind the high sensitivity of the electrical properties of NBT on A-site cation nonstoichiometry using a combination of advanced analytical techniques.[15,16] If the starting composition is stoichiometric, slightly Bi-deficient or Na excess, the final composition in the processed ceramics is Bi-deficient, leading to oxygen vacancies and oxide ion conduction.[15,16] In starting compositions with Bi excess, the Bi vacancies and oxygen vacancies (and therefore oxide ion conduction) are supressed[15] and insulating behaviour with near intrinsic electronic conduction is observed. In starting compositions

a)Author to whom correspondence should be addressed. Electronic mail: d.c.sinclair@sheffield.ac.uk

with Na deficiency, transmission electron microscopy (TEM) revealed the presence of TiO_2 secondary phase, suggesting the main phase is effectively a Bi-excess starting composition and therefore this composition is also insulating.[16] The two studies[15,16] provide guidelines on how to adjust the starting composition of NBT ceramics for dielectric/piezoelectric and oxide ion conductor applications.

Over the past decade, there has been a sharp increase in studies on NBT and related materials.[24–35] Most reports in the literature focus on optimisation of the dielectric and piezoelectric properties by developing solid solutions with other ferroelectric materials. There are few reports on the dielectric and piezoelectric properties in donor (Nb, Ta)-doped NBT.[36–39] Here, we report the effect on the electrical properties of Nb donor-doping on the Ti-site in NBT ceramics.

Compositions based on the general formula $Na_{0.5}Bi_{0.5}Ti_{1-x}Nb_xO_3$ ($x = 0.005$, 0.01, 0.02, and 0.03) were prepared using the solid state reaction method. Raw materials were predried before weighing and appropriate mixtures of powders were ball milled. Calcination was carried out at 800 °C with a further heat treatment at 850 °C, both for 2 h each. Pellets were sintered at 1150 °C for 2 h. More details can be found in previous reports.[15,16] Phase purity was examined by X-ray diffraction (XRD) using a high-resolution STOE STADI-P diffractometer equipped with a linear position sensitive detector and operated with Cu $K\alpha_1$ radiation. Ceramic microstructure and compositional analysis were performed using a scanning electron microscope (SEM) JEOL 6400 equipped with an Oxford Link ISIS energy dispersive x-ray spectroscopy (EDS) detector. High temperature Impedance Spectroscopy (IS) measurements were performed in a non-inductively wound tube furnace using an Agilent E4980A, an HP 4192A impedance analyser, and a Solartron 1260 system. Au paste (fired at 800 °C for 2 h) electrodes were used, and IS data were corrected for sample geometry (thickness/area of pellet) and analysed using ZView software. Polarisation-Electric field (P-E) measurements were performed using an aixACCT TF Analyzer 2000 E system.

Similar to that observed in the previous report,[36] the Nb-doping limit in $Na_{0.5}Bi_{0.5}Ti_{1-x}Nb_xO_3$ is low. XRD and SEM/EDS data (not shown) reveal the presence of small amount of $Bi_2Ti_2O_7$-related secondary phase for $x \geq 0.02$. However, even 1 at. %, Nb-doping significantly increases the bulk resistivity (R_b) at 600 °C from ~800 Ω cm for undoped NBT to ~620 kΩ cm, as shown by the diameter of the high frequency arc in the impedance complex plane (Z*) plots, Fig. 1(a). A typical Z* plot for $x = 0.01$ at 600 °C consists of a single arc with an associated capacitance (C) of ~88 pF cm^{-1}, corresponding to $\varepsilon_r \sim 994$. The high ε_r value is consistent with the ferroelectric behaviour of NBT, confirming that the arc is associated with the grain (bulk) response. The Z* plot of undoped NBT at 600 °C in air (see Figs. 2(a) and 2(b) in Ref. 15) consists of bulk, grain boundary, and electrode responses. With 1 at. % Nb doping, the ceramic becomes electrically homogeneous, as shown by the frequency coincidence for the Z″ and M″ Debye peak maximum in the combined spectroscopic plot, Fig. 1(b).

The Z* plot at 700 °C under different atmospheres for the Nb-doped ceramic shows R_b decreases with measuring pO_2 from ~56 kΩ cm in flowing O_2 (equilibrium period ~11 h) to

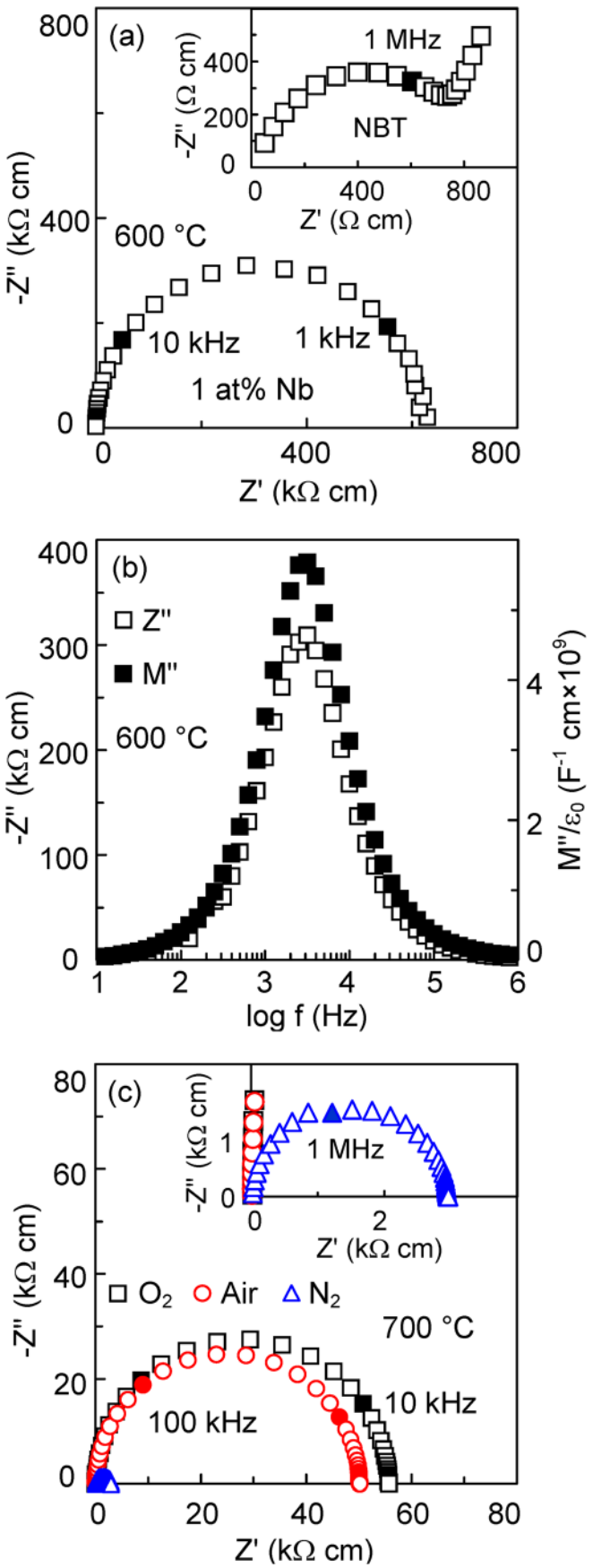

FIG. 1. (a) Z* plots and (b) combined Z″ and M″ spectroscopic plots of $x = 0.01$ at 600 °C. Inset in (a) shows the bulk response of undoped NBT ($x = 0$) on an expanded scale. (c) Z* plots for $x = 0.01$ at 700 °C under different atmospheres. Inset shows the data for measurements in N_2 on an expanded scale. Filled symbols indicate selected frequencies.

~3 kΩ cm in N_2 (equilibrium period ~25 h), Fig. 1(c). IS measurements were performed down to 0.01 Hz, and there was no clear evidence for the presence of a spike and/or arc associated with Warburg diffusion and oxide ion conduction in the Nb-doped ceramic. The pO_2 dependence of R_b and absence of any low frequency Warburg response suggests the dominance of n-type electronic conduction in the Nb-doped sample.

The temperature dependence of R_b for all samples is summarised in an Arrhenius plot of the bulk conductivity (σ_b), where $\sigma_b = 1/R_b$, Fig. 2. Clearly, R_b is very sensitive to Nb-doping and increases by more than three orders of magnitude at temperatures $\leq 500\,^{\circ}C$ and E_a increases to ~1.5 eV with only 0.5 at. % Nb doping. E_a increases to ~1.8 eV at higher doping levels. An E_a of 1.5–1.8 eV is about half the optical band gap of ~3.0–3.5 eV reported in the literature,[40–42] suggesting that the electronic conduction is close to intrinsic (band gap) behaviour.

The relative permittivity maximum ($\varepsilon_{r,max}$) decreases from ~3000 for undoped NBT to ~2800 for $x = 0.005$ and 0.01, Fig. 3(a). Further increasing of x to 0.02 and 0.03 decreases $\varepsilon_{r,max}$ to ~2400; however, the temperature of $\varepsilon_{r,max}$ (T_{max}) is similar for all samples. A significant change is observed for the dielectric loss ($\tan\delta$), where it increases sharply above ~300 °C for undoped NBT due to the high level of oxide-ion conductivity, Fig. 3(b). In contrast, Nb-doped samples exhibit $\tan\delta < 0.005$ at 300–600 °C, Figs. 3(b) and 3(c). The loss peak maximum shifts to lower temperature from ~220 °C for undoped NBT to ~125°–130° for $x = 0.005$ and 0.01 and to 80–90 °C for $x = 0.02$ and 0.03, Fig. 3(b).

Careful examination of loss data at ~500 °C reveals there is another loss peak in $x = 0.01$–0.03. A highest loss peak maximum of ~0.005 is observed for $x = 0.03$. In less resistive samples, such a loss peak, if present, will be masked by the high loss background associated with high leakage current and is therefore not observable. NBT exhibits a tetragonal-cubic phase transition at ~500–540 °C.[43,44] We speculate the loss peak at ~500 °C is associated with the tetragonal-cubic phase transition. Further study is needed to confirm the origin of this loss peak.

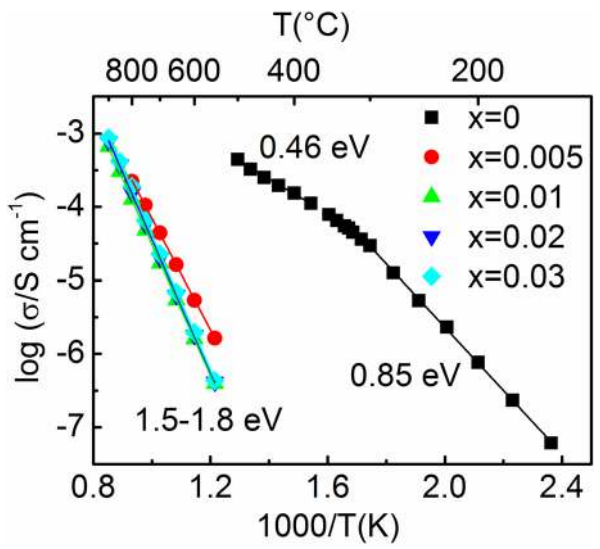

FIG. 2. Arrhenius-type plots of bulk conductivity for all $Na_{0.5}Bi_{0.5}Ti_{1-x}Nb_xO_3$ samples.

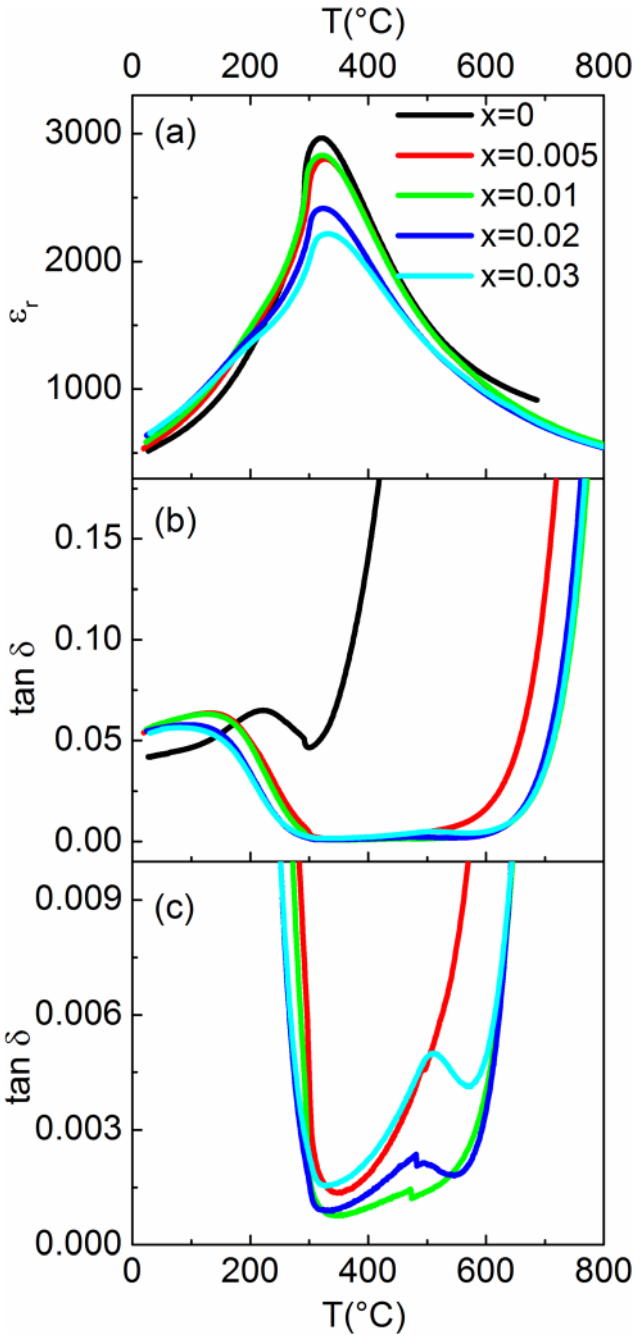

FIG. 3. Temperature dependence of (a) ε_r and (b) $\tan\delta$ at 1 MHz. (c) Expanded view of $\tan\delta$ at 300–600 °C for all $Na_{0.5}Bi_{0.5}Ti_{1-x}Nb_xO_3$ samples.

Hysteresis loops from P-E measurements show Nb-doping to influence the remanent polarization (P_r) and coercive field (E_c), Fig. 4. P_r initially increases from 38.8 μC/cm^2 for undoped NBT to 40.2 μC/cm^2 for $x = 0.005$ and to 42.8 μC/cm^2 for $x = 0.01$, then it decreases to 37.8 μC/cm^2 for $x = 0.02$ and 34.5 μC/cm^2 for $x = 0.03$. E_c decreases with increasing x, from ~53 kV/cm for undoped NBT to ~37 kV/cm for $x = 0.03$.

The IS results reveal NBT ceramics become significantly more resistive and electrically homogeneous with low levels of Nb-doping, Figs. 1 and 2. This behaviour is strikingly different from that commonly observed in $(Ba,Sr)TiO_3$-related titanates,[2,6,7] where low levels of donor-doping can induce substantial levels of semiconductivity. In

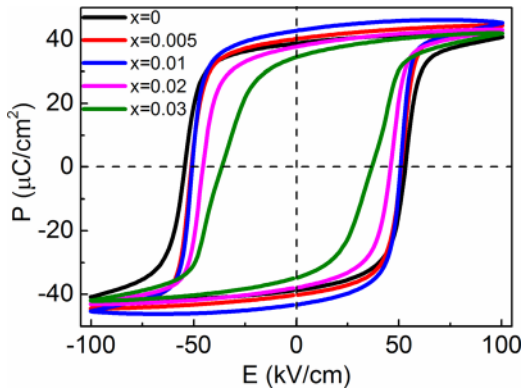

FIG. 4. Polarisation-electric field (P-E) hysteresis loops measured at 0.1 Hz and up to 100 kV/cm for all $Na_{0.5}Bi_{0.5}Ti_{1-x}Nb_xO_3$ samples.

the previous studies,[15,16] we confirmed that the high leakage current in NBT is associated with oxide ion conduction rather than electronic conduction. Bismuth and oxygen vacancies are generated through a loss of a small amount of Bi_2O_3 during ceramic processing, as given in the following Kroger-Vink equation

$$2\,Bi_{Bi}^{\times} + 3O_O^{\times} \rightarrow 2\,V_{Bi}''' + 3V_O^{\bullet\bullet} + Bi_2O_3. \quad (1)$$

Donor-doping (such as Nb^{5+} at Ti-site) can fill up the oxygen vacancies according to the equation

$$Nb_2O_5 + V_O^{\bullet\bullet} \rightarrow 2Nb_{Ti}^{\bullet} + 5O_O^{\times}. \quad (2)$$

The overall reaction is

$$2Bi_{Bi}^{\times} + 3O_O^{\times} + 3Nb_2O_5 \rightarrow 2V_{Bi}''' + 6Nb_{Ti}^{\bullet} + 15O_O^{\times} + Bi_2O_3. \quad (3)$$

Thus, the oxide ion conductivity is suppressed and Nb-doped ceramics exhibit near intrinsic electronic conduction. This ionic compensation doping mechanism in Nb-doped NBT is different from the electronic compensation commonly observed in donor-doped (Ba,Sr)TiO_3. The donor doping mechanisms in (Ba,Sr)TiO_3 are complex[2,12–14] and depend on various factors including sintering temperature, atmosphere, cooling rate, doping level, A/B ratio, and dopant ion size. Here, we compare the electrical properties of Nb-doped NBT and donor doped (Ba,Sr)TiO_3 prepared at temperatures required to obtained dense ceramics (~1150 °C for NBT and ~1350 °C for (Ba,Sr)TiO_3) with a common cooling rate (5°/min).

A further contributing factor is the difference in their band structures. The $6s^2$ electron lone pairs associated with the Bi-ions are involved in hybridisation with the 2 p orbitals associated with the O-ions, and therefore, the valence band in NBT has significant cation character. In (Ba,Sr)TiO_3, there are no electron lone pairs associated with the A-site cations and the valence band is based mainly on anion character. As shown by Klein *et al.*,[45] this influences the relative energy levels of the valence and conduction bands. In particular, the lone-pair effect in NBT produces a high valence band maximum and high conduction band minimum that does not favour the formation of Nb electronic donor-states and high levels of n-type electronic conductivity in Nb-doped NBT.

The Bi_2O_3 loss in NBT during sample processing is "accidental" and therefore difficult to control in a reproducible manner. The loss is also very small and is challenging to quantify.[15,16] Equation (3) can be used to estimate the bismuth and oxygen vacancy concentration. Our results show that NBT (under the processing conditions employed in our studies) becomes highly resistive for $x = 0.005$–0.01 in $Na_{0.5}Bi_{0.5}Ti_{1-x}Nb_xO_3$. Based on Eq. (3), the bismuth and oxygen nonstoichiometry in NBT is in the range of 0.0017–0.0033 for bismuth and 0.0025–0.0050 for oxygen, corresponding to a formula of $Na_{0.5}Bi_{0.4967-0.4983}TiO_{2.995-2.9975}$. This demonstrates again the highly sensitive relationship between nonstoichiometry and electrical properties in NBT.

The extensive studies on NBT and related materials over the past decade have optimised solid solutions between NBT, $BaTiO_3$, and KNN for piezoelectric and high temperature capacitor applications.[24–33] The development history of (Ba,Sr)TiO_3-type devices[1–8] is based on the crucial importance of understanding the defect chemistry to optimise and accurately control the composition(s) with various donor and acceptor dopants for better performance, low cost and reproducible, large scale manufacturing. This work and our previous studies[15,16] show that NBT has a different defect chemistry to (Ba,Sr)TiO_3 and is presumably linked to small but significant variations in A-site non-stoichiometry in NBT that does not exist to the same extent in (Ba,Sr)TiO_3-based systems. The knowledge of defect chemistry accumulated for (Ba,Sr)TiO_3 cannot therefore be applied directly to NBT-related materials. Clearly, more systematic work on the defect chemistry of donor and acceptor doping in NBT-based solid solutions is needed prior to any large scale industrial manufacturing of NBT-based devices in the near future.

We thank the EPSRC for funding EP/L027348/1.

[1]A. J. Moulson and J. M. Herbert, *Electroceramics: Materials, Properties, Applications*, 2nd ed. (John Wiley and Sons Ltd., 2003).
[2]D. M. Smyth, *The Defect Chemistry of Metal Oxides* (Oxford University Press, New York, 2000).
[3]I. Burn and G. H. Maher, J. Mater. Sci. **10**, 633 (1975).
[4]Y. H. Han, J. B. Appleby, and D. M. Smyth, J. Am. Ceram. Soc. **70**, 96 (1987).
[5]H. Kishi, Y. Mizuno, and H. Chazono, Jpn. J. Appl. Phys., Part 1 **42**, 1 (2003).
[6]O. Saburi, J. Phys. Soc. Jpn. **14**, 1159 (1959).
[7]G. H. Jonker, Solid-State Electron. **7**, 895 (1964).
[8]B. Huybrechts, K. Ishizaki, and M. Takata, J. Mater. Sci. **30**, 2463 (1995).
[9]T. Tomio, H. Miki, H. Tabata, T. Kawai, and S. Kawai, J. Appl. Phys. **76**, 5886 (1994).
[10]S. Ohta, T. Nomura, H. Ohta, and K. Koumoto, J. Appl. Phys. **97**, 034106 (2005).
[11]D. Neagu and J. T. S. Irvine, Chem. Mater. **22**, 5042 (2010).
[12]F. D. Morrison, D. C. Sinclair, and A. R. West, J. Appl. Phys. **86**, 6355 (1999).
[13]C. L. Freeman, J. A. Dawson, H. Ru. Chen, J. H. Harding, L. B. Ben, and D. C. Sinclair, J. Mater. Chem. **21**, 4861 (2011).
[14]I. Akin, M. Li, Z. Lu, and D. C. Sinclair, RSC Adv. **4**, 32549 (2014).
[15]M. Li, M. J. Pietrowski, R. A. De Souza, H. Zhang, I. M. Reaney, S. N. Cook, J. A. Kilner, and D. C. Sinclair, Nat. Mater. **13**, 31 (2014).
[16]M. Li, H. Zhang, S. N. Cook, L. Li, J. A. Kilner, I. M. Reaney, and D. C. Sinclair, Chem. Mater. **27**, 629 (2015).
[17]M. Spreitzer, M. Valant, and D. Suvorov, J. Mater. Chem. **17**, 185 (2007).
[18]H. Nagata, J. Ceram. Soc. Jpn. **116**, 271 (2008).

[19]Y. Noguchi, I. Tanabe, M. Suzuki, and M. Miyayama, J. Ceram. Soc. Jpn. **116**, 994 (2008).
[20]R. Z. Zuo, S. Su, Y. Wu, J. Fu, M. Wang, and L. T. Li, Mater. Chem. Phys. **110**, 311 (2008).
[21]Y. S. Sung, J. M. Kim, J. H. Cho, T. K. Song, M. H. Kim, H. H. Chong, T. G. Park, D. Do, and S. S. Kim, Appl. Phys. Lett. **96**, 022901 (2010).
[22]Y. S. Sung, J. M. Kim, J. H. Cho, T. K. Song, M. H. Kim, and T. G. Park, Appl. Phys. Lett. **98**, 012902 (2011).
[23]J. Carter, E. Aksel, T. Iamsasri, J. S. Forrester, J. Chen, and J. L. Jones, Appl. Phys. Lett. **104**, 112904 (2014).
[24]Y. Hiruma, H. Nagata, and T. Takenaka, J. Appl. Phys. **105**, 084112 (2009).
[25]T. R. Shrout and S. J. Zhang, J. Electroceram. **19**, 113 (2007).
[26]T. Takenaka, H. Nagata, and Y. Hiruma, Jpn. J. Appl. Phys., Part 1 **47**, 3787 (2008).
[27]J. Rödel, W. Jo, K. T. P. Seifert, E. M. Anton, T. Granzow, and D. Damjanovic, J. Am. Ceram. Soc. **92**, 1153 (2009).
[28]X. X. Wang, X. G. Tang, and H. L. W. Chan, Appl. Phys. Lett. **85**, 91 (2004).
[29]S. T. Zhang, A. B. Kounga, E. Aulbach, T. Granzow, W. Jo, H.-J. Kleebe, and J. Rödel, J. Appl. Phys. **103**, 034107 (2008).
[30]E. A. Patterson, D. P. Cann, J. Pokorny, and I. M. Reaney, J. Appl. Phys. **111**, 094105 (2012).
[31]R. Dittmer, E.-M. Anton, W. Jo, H. Simons, J. E. Daniels, M. Hoffman, J. Pokorny, I. M. Reaney, and J. Rödel, J. Am. Ceram. Soc. **95**, 3519 (2012).
[32]J. Zang, W. Jo, H. Zhang, and J. Rödel, J. Eur. Ceram. Soc. **34**, 37 (2014).
[33]E. Sapper, R. Dittmer, D. Damjanovic, E. Erdem, D. J. Keeble, W. Jo, T. Granzow, and J. Rödel, J. Appl. Phys. **116**, 104102 (2014).
[34]J. Zang, M. Li, D. C. Sinclair, T. Frömling, W. Jo, and J. Rödel, J. Am. Ceram. Soc. **97**, 2825 (2014).
[35]W. W. Ge, C. T. Luo, Q. H. Zhang, Y. Ren, J. F. Li, H. S. Luo, and D. Viehland, Appl. Phys. Lett. **105**, 162913 (2014).
[36]H. G. Yeo, Y. S. Sung, T. K. Song, J. H. Cho, M. H. Kim, and T. G. Park, J. Korean Phys. Soc. **54**, 896 (2009).
[37]R. Zuo, H. Wang, B. Ma, and L. Li, J. Mater. Sci.: Mater. Electron. **20**, 1140 (2009).
[38]K. Kumar and B. Kumar, Ceram. Int. **38**, 1157 (2012).
[39]N. Petnoi, P. Bomlai, S. Jiansirisomboon, and A. Watcharapasorn, Ceram. Int. **39**, S113 (2013).
[40]M. Bousquet, J. R. Duclere, E. Orhan, A. Boulle, C. Bachelet, and C. Champeaux, J. Appl. Phys. **107**, 104107 (2010).
[41]C. Y. Kim, T. Sekino, and K. Niihara, J. Sol-Gel Sci. Technol. **55**, 306 (2010).
[42]M. Zeng, S. W. Or, and H. L. W. Chan, J. Appl. Phys. **107**, 043513 (2010).
[43]G. O. Jones and P. A. Thomas, Acta Crystallogr., Sect. B: Struct. Sci. **58**, 168 (2002).
[44]G. Trolliard and V. Dorcet, Chem. Mater. **20**, 5074 (2008).
[45]S. Y. Li, J. Morasch, A. Klein, C. Chirila, L. Pintilie, L. C. Jia, K. Ellmer, M. Naderer, K. Reichmann, M. Gröting, and K. Albe, Phys. Rev. B **88**, 045428 (2013).